Supplementary Materials

Plasmonic photocatalysts Au/g-C_3N_4/$NiFe_2O_4$ nanocomposites for enhanced visible-light-driven photocatalytic hydrogen evolution

Jian Zeng [a], Ting Song [a], Meixiang Lv [a], Tingting Wang [b], Jiayi Qin [a] and Heping Zeng *[a,b]

[a] Guangzhou Key Laboratory of Materials for Energy Conversion and Storage, School of Chemistry and Environment, South China Normal University, Guangzhou, 510006, P. R. China.

[b] State Key Laboratory of Luminescent Materials and Devices, Institute of Functional Molecules, School of Chemistry and Chemical Engineering, South China University of Technology, Guangzhou, 510641, P. R. China.

Corresponding author: Tel: +86-20-87112631; Fax: +86-20-87112631; E-mail: hpzeng@scut.edu.cn;

Fig. S1 Photocatalytic hydrogen evolution testing system.

Fig. S2 XRD patterns of a series of $NiFe_2O_4$/g-C_3N_4 (a) and Au/$NiFe_2O_4$/g-C_3N_4 nanocomposites (b).

Fig. S3 FT-IR spectra of a series of $NiFe_2O_4$/g-C_3N_4 nanocomposites, g-C_3N_4 and $NiFe_2O_4$, respectively.

Fig. S4 Elemental mapping of 1.0 wt% Au/4NFCN.

Fig. S5 The XPS spectra survey of 1.0 wt% Au/4NFCN.

Fig. S6 The band gap value of $NiFe_2O_4$, g-C_3N_4, 4NFCN, 1.0 wt% Au/$NiFe_2O_4$, 1.0 wt% Au/g-C_3N_4 and 1.0 wt% Au/4NFCN was estimated by Kubelka-Munk equation.

Fig. S7 The UV-vis images of a series of g-C_3N_4/$NiFe_2O_4$ nanocomposites and Au/g-C_3N_4/$NiFe_2O_4$ nanocomposites.

Fig. S8 GC Chromatogram of hydrogen production by the representative photocatalysts.

Figure. S9 The XRD patterns of 1.0 wt% Au/4NFCN before and after the stability test.

Figure. S10 The VB XPS of pure $NiFe_2O_4$ and pure g-C_3N_4.

Fig. S11 The PL spectra of g-C_3N_4/$NiFe_2O_4$ and Au/g-C_3N_4/$NiFe_2O_4$ nanocomposites.

Fig. S12 Transient photocurrent responses g-C_3N_4/$NiFe_2O_4$ and Au/g-C_3N_4/$NiFe_2O_4$ nanocomposites.

Determination of AQY values

Table S1 The hydrogen evolution rate, S_{BET}, pore volume and average pore size of as-prepared samples.

Fig. S1 Photocatalytic hydrogen evolution testing system.

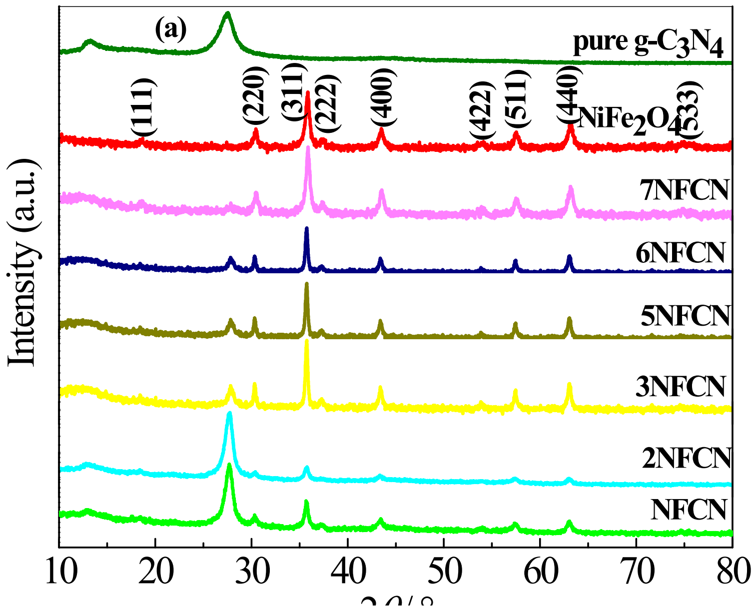

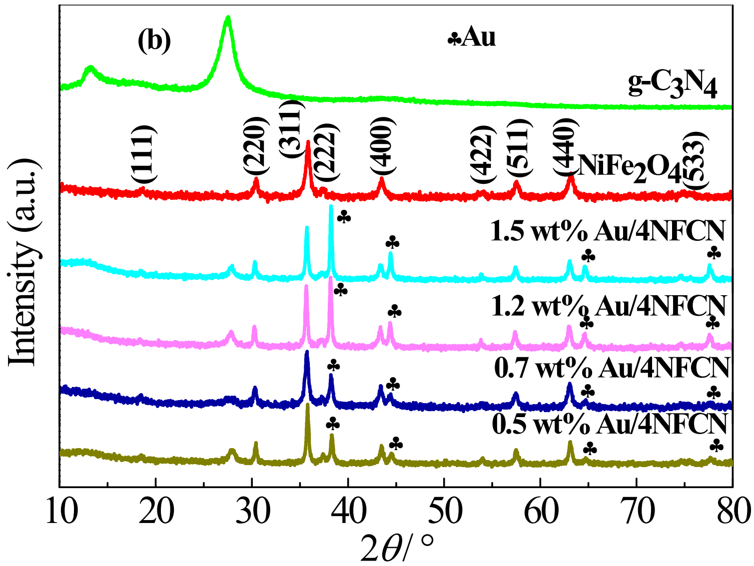

Fig. S2 XRD patterns of a series of g-C_3N_4/$NiFe_2O_4$ (a) and Au/g-C_3N_4/$NiFe_2O_4$ nanocomposites (b).

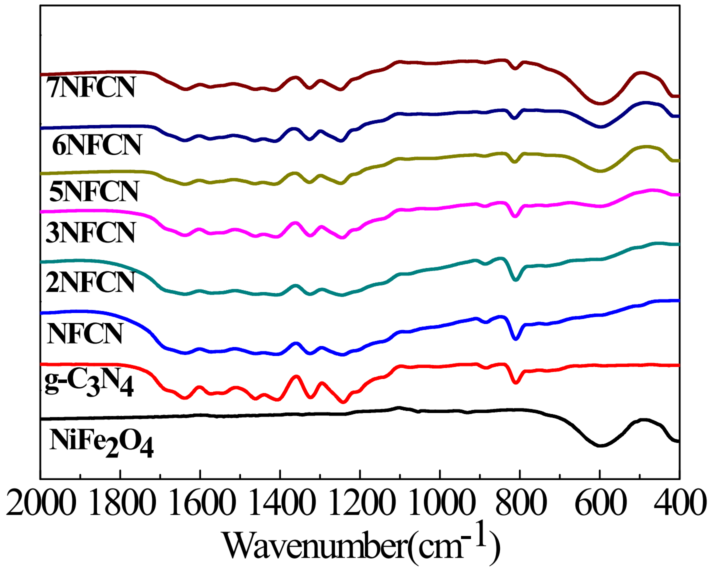

Fig. S3 FT-IR spectra of a series of g-C_3N_4/$NiFe_2O_4$ nanocomposites, g-C_3N_4 and $NiFe_2O_4$, respectively.

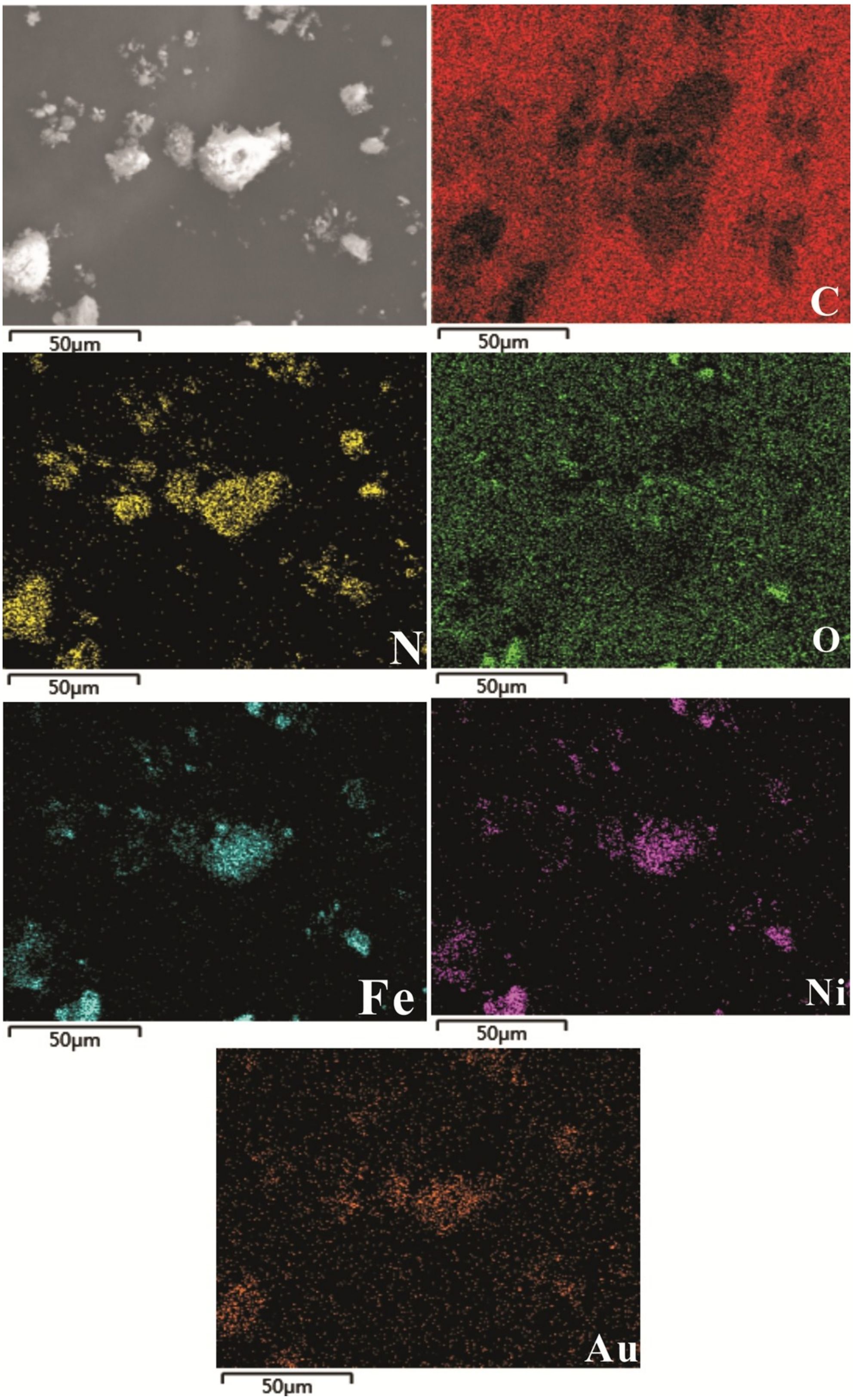

Fig. S4 Elemental mapping of 1.0 wt% Au/4NFCN.

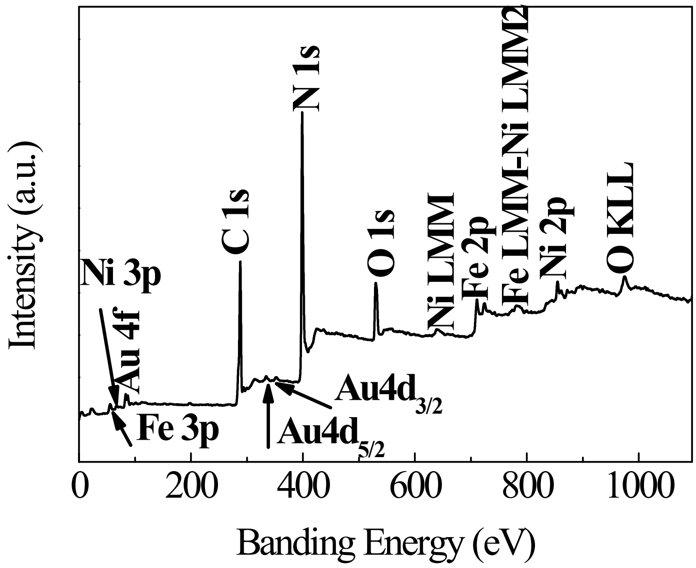

Fig. S5 The XPS spectra survey of 1.0 wt% Au/4NFCN.

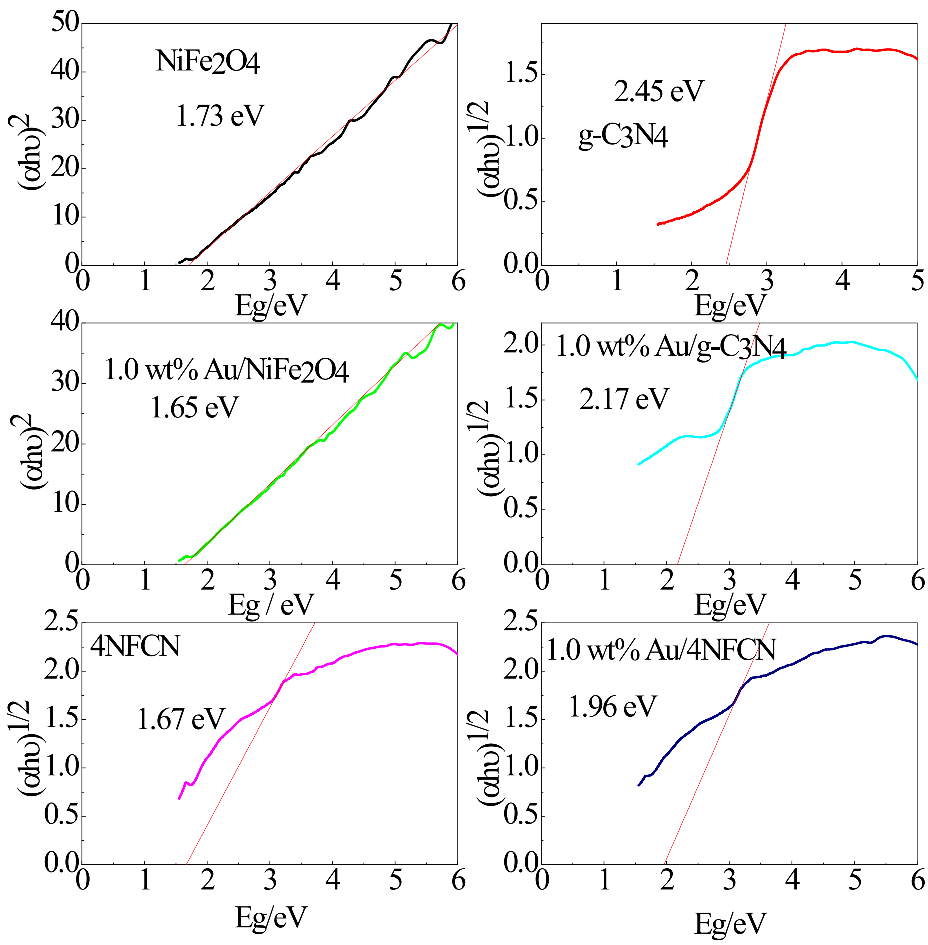

Fig. S6 The band gap value of $NiFe_2O_4$, $g\text{-}C_3N_4$, 4NFCN, 1.0 wt% Au/$NiFe_2O_4$, 1.0 wt% Au/$g\text{-}C_3N_4$ and 1.0 wt% Au/4NFCN was estimated by Kubelka-Munk equation.

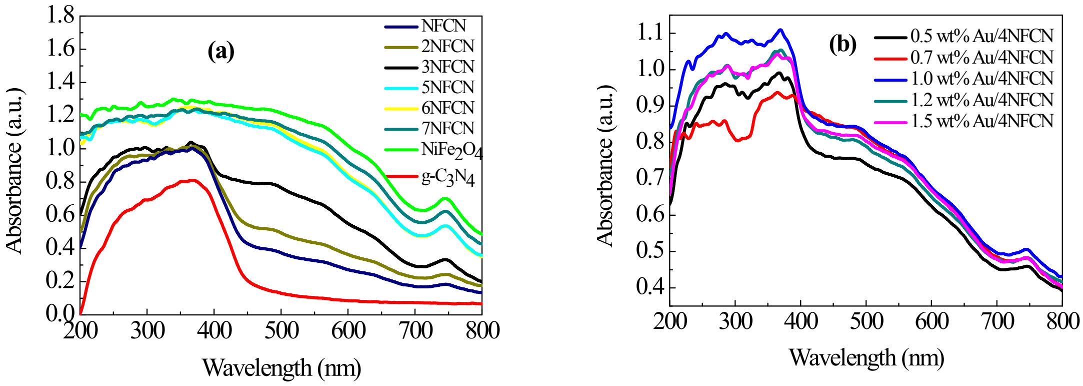

Fig. S7 The UV-vis images of a series of g-C_3N_4/$NiFe_2O_4$ nanocomposites and Au/g-C_3N_4/$NiFe_2O_4$ nanocomposites.

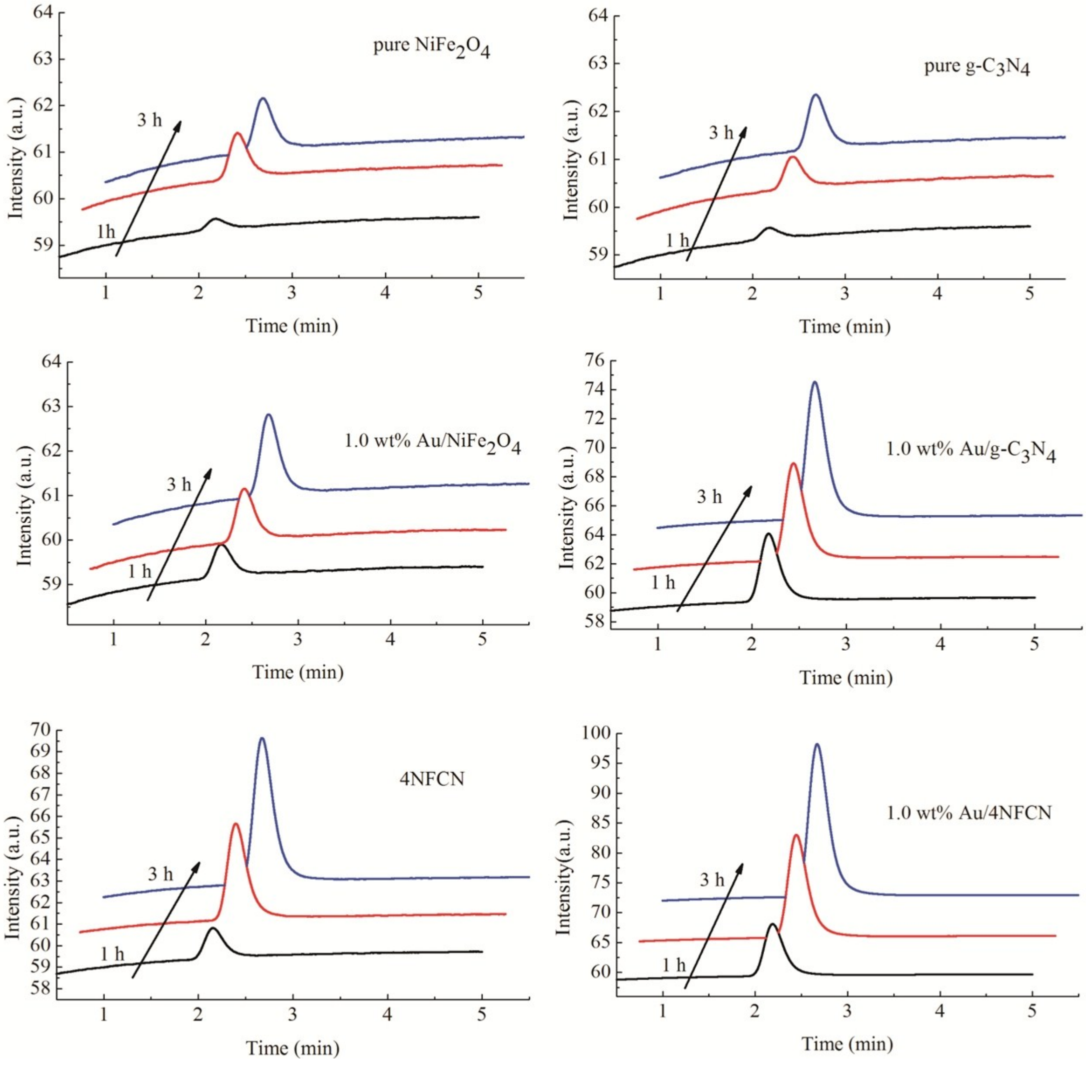

Fig. S8 GC Chromatogram of hydrogen production by the representative photocatalysts.

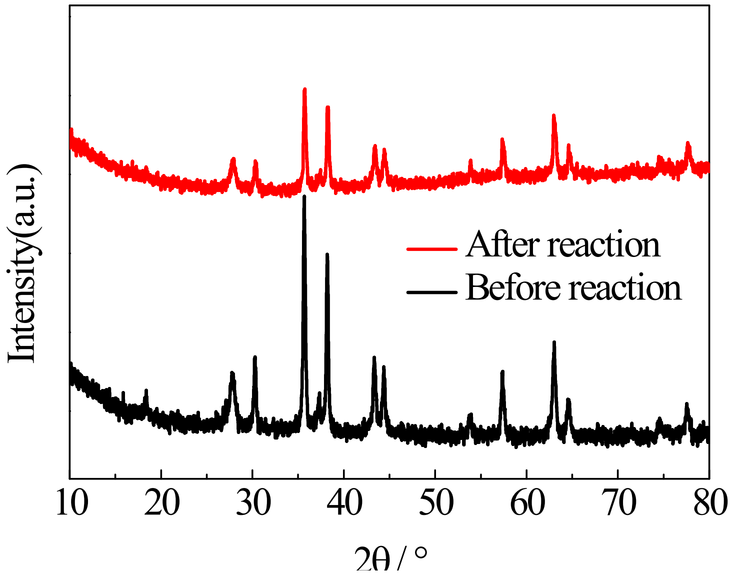

Figure. S9 The XRD patterns of 1.0 wt% Au/4NFCN before and after the stability test.

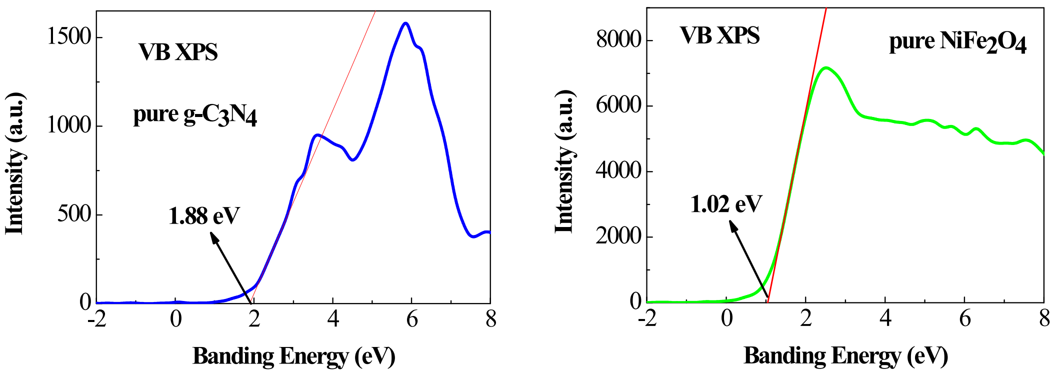

Figure. S10 The VB XPS of pure $NiFe_2O_4$ and pure $g\text{-}C_3N_4$.

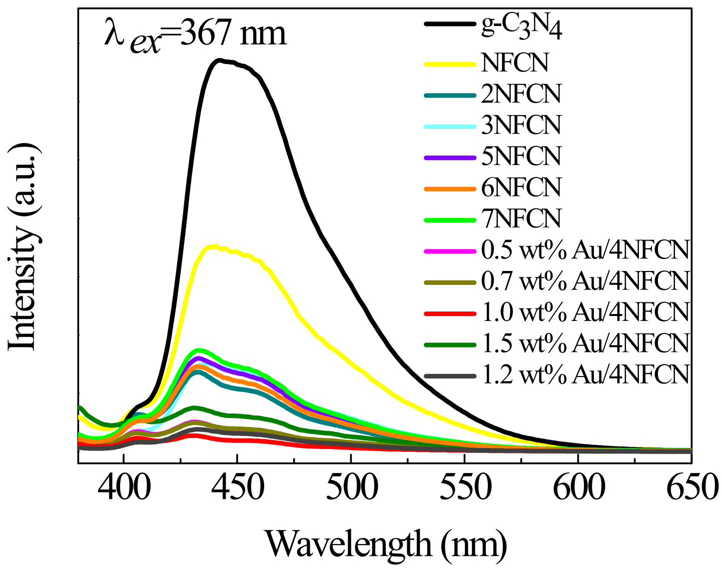

Fig. S11 The PL spectra of $g\text{-}C_3N_4/NiFe_2O_4$ and $Au/g\text{-}C_3N_4/NiFe_2O_4$ nanocomposites.

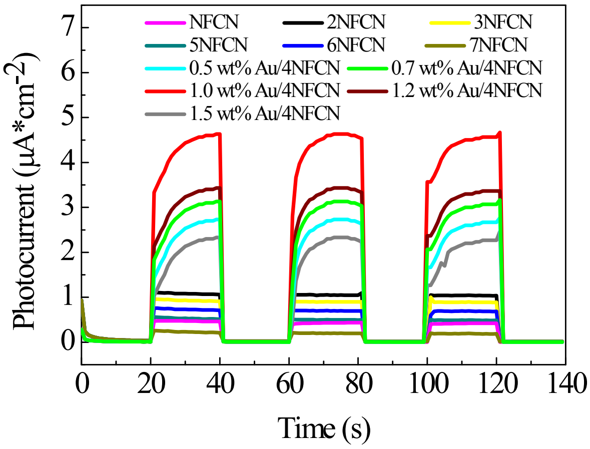

Fig. S12 Transient photocurrent responses g-C_3N_4/$NiFe_2O_4$ and Au/g-C_3N_4/$NiFe_2O_4$ nanocomposites.

Determination of AQY values[1]

Apparent quantum efficiency (AQY) was measured under identical photoreaction conditions except that the incident monochromatic light with a band-pass filter (λ = 420 nm, half width =15 nm) and an irradiatometer. The hydrogen yields of 1 h photocatalytic reaction in one continuous reaction under visible light with the wavelength of 420 nm were measured. The incident photon number was determined by a calibrated Si photodiode (SRC-1000-TC-QZ-N, Oriel), and the AQY value was calculated using eqn (1).

$$\text{AQY (\%)} = \frac{2\times\text{Number of evolved } H_2 \text{ molecules}}{\text{Number of incident photos}} \times 100\% \quad (1)$$

Table S1 the elemental composition of 1.0 wt% Au/4NFCN.

Elemental	C	N	O	Fe	Ni	Au
Wt%	20.84	11.09	15.49	39.36	12.20	1.01
At%	39.32	17.95	21.94	15.97	4.71	0.12

Reference

1. J. P. Huo, H. P. Zeng, *J. Mater. Chem. A*, 2015, **3**, 6258.